

# Brain-controlled Assistive Robotics and Prosthetics

Kavya Puthuveetil and Dean J. Krusienski

Department of Biomedical Engineering, Virginia Commonwealth University,  
Richmond, VA, USA

Dean J. Krusienski, Ph.D.

Professor of Biomedical Engineering

Virginia Commonwealth University

Richmond, VA

[djkrusienski@vcu.edu](mailto:djkrusienski@vcu.edu)

Kavya Puthuveetil

Biomedical Engineering

Virginia Commonwealth University

Richmond, VA

# Contents

<b>1</b>	<b>Introduction</b>	<b>1</b>
<b>2</b>	<b>Brain-Computer/Brain-Machine Interfaces</b>	<b>1</b>
<b>3</b>	<b>Applications to Assistive Robotics and Prosthetics</b>	<b>12</b>
<b>4</b>	<b>Artificial Intelligence and Shared Control</b>	<b>19</b>
<b>5</b>	<b>Current Challenges and Future Prospects</b>	<b>22</b>

## Abstract

This chapter provides an overview of prior and prospective work related to the control of assistive robotics and prostheses via direct measurements of brain activity. Specifically, this chapter focuses on brain-controlled robotic devices that *replace*, *supplement*, or *restore* lost motor function. The chapter introduces noninvasive and invasive brain signal recording modalities, common brain-actuated control signals, and a survey of applications in assistive robotics and prosthetics. The chapter concludes with a discussion of current challenges and future prospects of these technologies.

**Keywords:** brain-computer interface, brain-machine interface, electroencephalogram, action potentials, electrodes, upper-limb prosthetics, orthotics, exoskeletons, wheelchairs, telepresence, assistive robots

# 1 Introduction

This chapter provides an overview of prior and prospective work related to the control of assistive robotics and prostheses via direct measurements of brain activity. Specifically, this chapter focuses on brain-controlled robotic devices that *replace*, *supplement*, or *restore* lost motor function [100]. The chapter does not include brain-controlled robotic devices that have been developed for rehabilitation or therapeutic applications, which are included in Chapter 6. The present chapter introduces noninvasive and invasive brain signal recording modalities, common brain-actuated control signals, and a survey of applications in assistive robotics and prosthetics. The chapter concludes with a discussion of current challenges and future prospects of these technologies.

## 2 Brain-Computer/Brain-Machine Interfaces

A brain-computer interface (BCI) is a system that directly translates neuronal signals into actionable inputs for an external device, as shown in Figure 1. The term BCI is generally synonymous with brain-machine interface (BMI), with the terms emerging from the noninvasive and invasive research communities, respectively. This general field of research originated as a means to help severely disabled individuals (e.g., suffering from late-stage amyotrophic lateral sclerosis (ALS) or brainstem stroke) communicate and perform tasks of daily living [98]. While the field has since evolved to include other non-medical applications, there is still significant focus on medical applications of BCI.

Because the impetus for BCIs was to restore, replace, or supplement lost function, much of the early work was focused on controlling motor prostheses, orthotics, and assistive devices [81]. Ideally, the ultimate objective is to completely restore natural motor function that has been lost by the user. However, approaching such naturalistic and transparent control in practice requires precise measurement of large-scale neural activity that can currently only be achieved via invasive measurements of brain activity (e.g., surgical implantation of high-

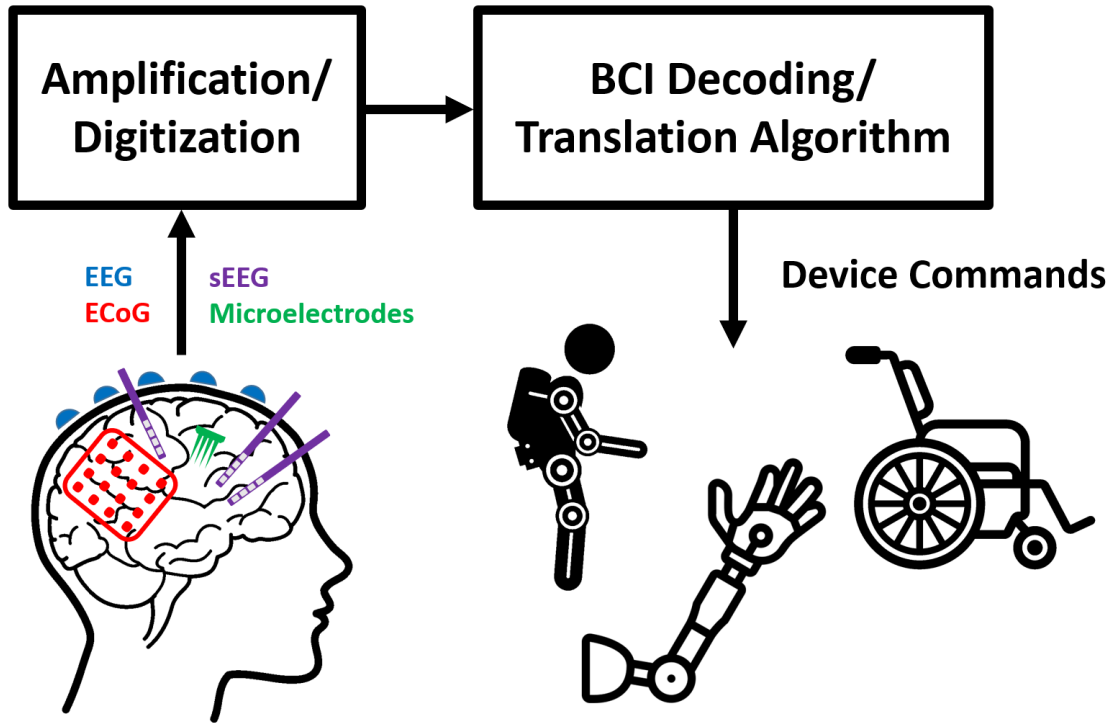


Figure 1: Block diagram of a brain-computer interface (BCI).

density electrodes into the brain).

Due to the inherent risks of surgical implants, much of the research has been conducted in animal models (primarily non-human primates [12, 13, 52, 95]) and, in special cases, on humans undergoing surgical procedures for intractable epilepsy and glioma removal [31, 78]. Additionally, there have been a limited number of long-term human implants exclusively for BCI research [17, 23, 27, 45, 96]. In contrast, current modalities for noninvasive measurement of brain activity cannot provide sufficient fidelity to achieve natural, refined control of a motor prosthetic. Nevertheless, the ability to control assistive devices with as few as 2-3 degrees of freedom, e.g., wrist rotation and hand grasp, has the potential to greatly improve the user's performance on activities of daily living [29].

Broadly, there are two classes of brain activity measurements that are relevant for such applications: (1) electrophysiological and (2) hemodynamic. Hemodynamic activity can be measured with functional magnetic resonance imaging (fMRI), positron emission tomography

(PET), and functional near-infrared imaging (fNIRS). Because of the comparatively slow hemodynamic response on the order of 1-2 seconds, and the impractical size and cost of the devices for independent daily use (in the case of fMRI and PET), these modalities are generally not well-suited for real-time robotic control applications.

Conversely, electrophysiological measurements of brain activity provide response times on the order of milliseconds and can be designed to be portable or fully-implantable, making them suitable for real-time control and independent daily use. The established modalities for invasively and noninvasively acquiring electrical brain activity for BCI applications are described below.

## 2.1 Invasive Recordings

There are three general categories of implanted electrodes, characterized by the method of implantation, depth of penetration, and size of the recording contacts. The most commonly used types of implanted electrodes are shown in Figures 2A-C.

### 2.1.1 Microelectrodes

Microelectrodes are penetrating electrodes designed to record from individual neurons, commonly referred to as *single units*. Most modern microelectrodes are configured as arrays of needle-like probes with electrodes along the shafts of each probe [14]. The electrodes generally have surface areas and spacings on the order of 1-10  $\mu\text{m}$  and are fabricated using silicon substrates. Individual microelectrode arrays are typically designed for sampling tens of hundreds [55, 89], and potentially thousands [41, 68], of neurons simultaneously.

Ideally, each microelectrode contact will measure action potentials from a single neuron. In practice, only a subset of contacts will yield clean recordings of action potentials from individual neurons. Otherwise, contacts can also measure local field potentials (LFPs), representing a superposition of electrical activity from surrounding neurons.

The acquisition of action potentials from a population of neurons in the motor cortex

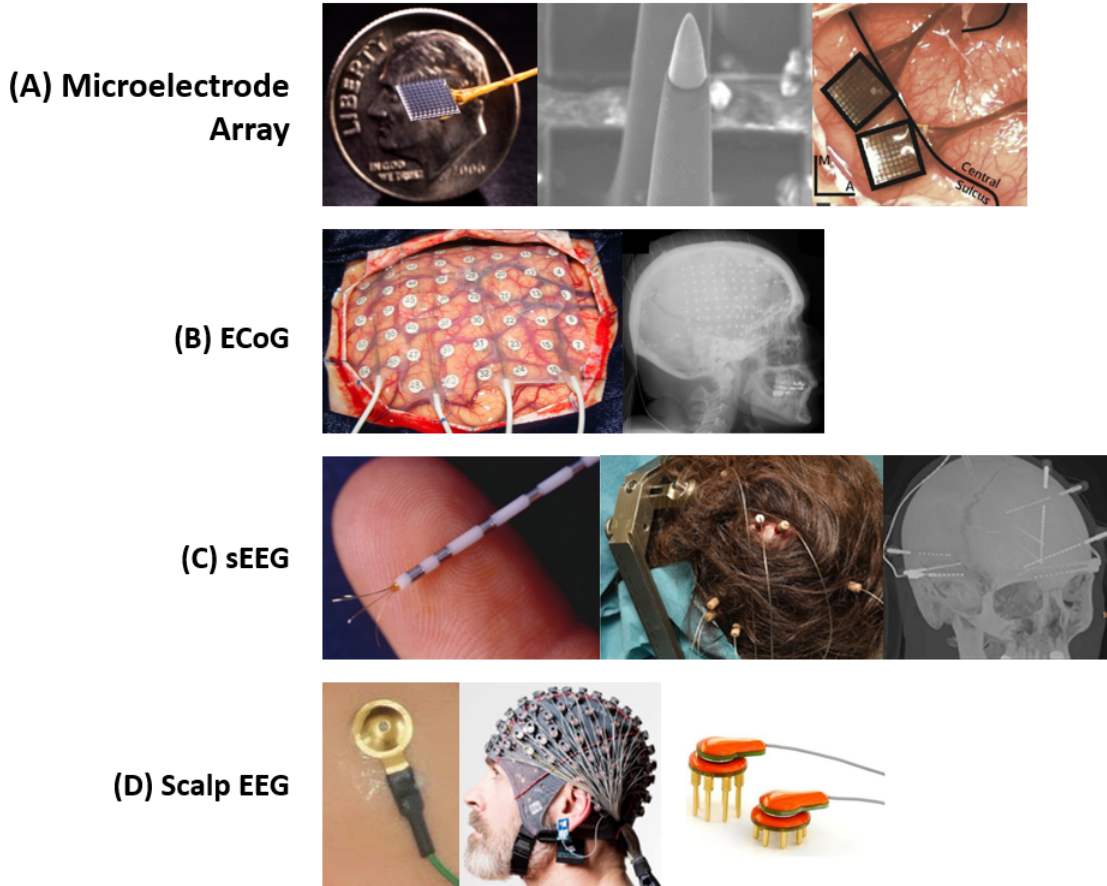


Figure 2: Types of invasive/noninvasive electrodes. (A) Microelectrode array; individual electrode tip; implanted electrode. (B) ECoG grid during craniotomy; post-op CT. (C) sEEG electrode with microwires at tip; view of scalp after implantation; post-op CT. (D) Wet EEG electrode; EEG electrode cap; dry EEG electrode.

can precisely determine movement intentions based on a phenomenon known as *population coding* [26]. Put simply, individual neurons in the motor cortex have been shown to have firing rates that follow a cosine tuning curve, where the firing rate of each neuron maximally corresponds to a preferred direction of movement and minimally corresponds to movements in the opposite direction (i.e., 180 degrees), with intermediate directions following a cosine curve (as shown in Figures 3 A-B). By sampling a sufficient number of neurons in the motor cortex, shown to be as few as 10-100 [33], continuous motor movements can be accurately reconstructed by taking the vector sum of the predicted movement directions for each neuron in the population as prescribed by the predetermined tuning curves (Figure 3C). Because the

resulting control signal represents a fairly direct mapping of the measured neuronal function, this approach yields naturalistic control of motor prostheses [17].

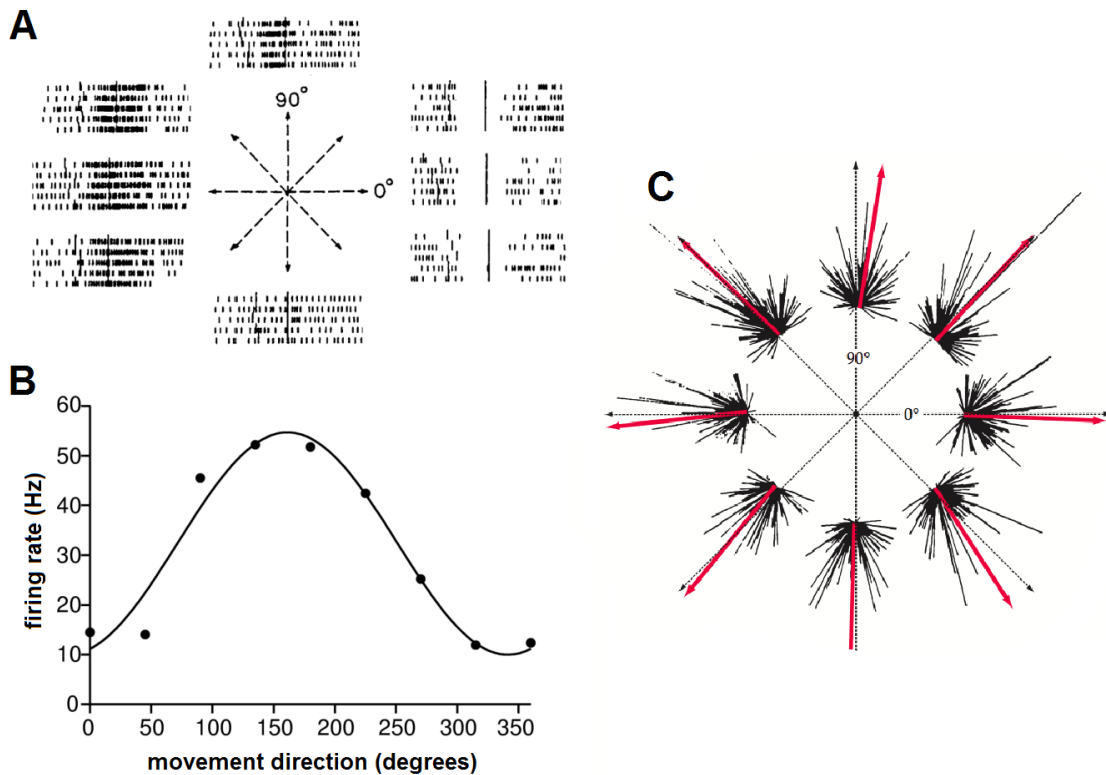


Figure 3: Population coding of cortical motor neurons. (A) Hand reaching directions and associated spike raster plots from a single neuron. (B) Corresponding cosine tuning curve for the neuron. (C) Predicted direction vectors (red) based on the individual tuning curves of a population of neurons. Adapted from [26].

### 2.1.2 ECoG and sEEG

Electrocorticography (ECoG) uses comparatively larger disk electrodes in rectangular arrays or strips placed on the cortical surface via a craniotomy [78]. The standard clinical electrodes are 5 mm in diameter with 1 cm spacing between contacts, although microECoG arrays also have been used with diameters and spacings on the order of tens of microns [43]. While ECoG does not penetrate the brain or record single unit activity, it can provide detailed information for decoding sensory, motor, and cognitive processes for a BCI. ECoG recording provide signals that are morphologically similar to LFPs with spectral bandwidth of roughly

0-250 Hz. ECoG is used clinically for localizing and mapping as part of surgical planning for intractable epilepsy and intraoperatively for glioma removal. To minimize the extent of the required craniotomy, ECoG grid placement is typically localized to particular cortical areas associated with the patient’s pathology, typically on a single hemisphere. For clinical purposes, the number of implanted ECoG electrodes typically ranges from 16-128, depending on the nature and location of the pathology.

A related technology employed for epileptic seizure localization is stereotactic EEG (sEEG) [31]. sEEG electrodes are positioned along a cylindrical shaft ( $\sim 1$  mm diameter), which is inserted deeper into the brain through small burr holes in the skull using stereotactic guidance. The surface area, number of electrodes implanted, and nature of the measured signals of sEEG for clinical purposes are roughly comparable to ECoG, although higher density contacts and microwires can be used. While, in contrast to ECoG, sEEG electrodes penetrate brain tissue, there is evidence that the procedures are as effective as ECoG and have improved surgical recovery outcomes compared to the craniotomy required for ECoG. Also, unlike the single, localized craniotomy for ECoG, the comparatively minute burr holes for sEEG electrodes allows for a broader but sparse sampling of both superficial and deeper brain structures. This creates a trade-off for investigating and utilizing specific brain regions and networks compared to the generally superior local cortical resolution provided by ECoG.

While the traditional lower-frequency rhythms can be observed in intracranial recordings, one unique and commonly used feature of ECoG/sEEG signals for BCI control is broadband gamma activity [62]. This activity manifests as roughly uniform fluctuations in the signal spectrum over the approximate range of 70-250 Hz, which resembles a broadband noise process and is not practically observable in scalp EEG, as illustrated in Figure 4. This activity has been shown to be highly correlated with a wide variety of cognitive and behavioral function. It is important to note that, while high frequency oscillations exist, broadband gamma is generally not considered a brain oscillation akin to lower frequency gamma ( $\sim 40$ -70 Hz) or the traditional lower-frequency EEG bands below 40 Hz (i.e., delta, theta, alpha,

beta)[64].

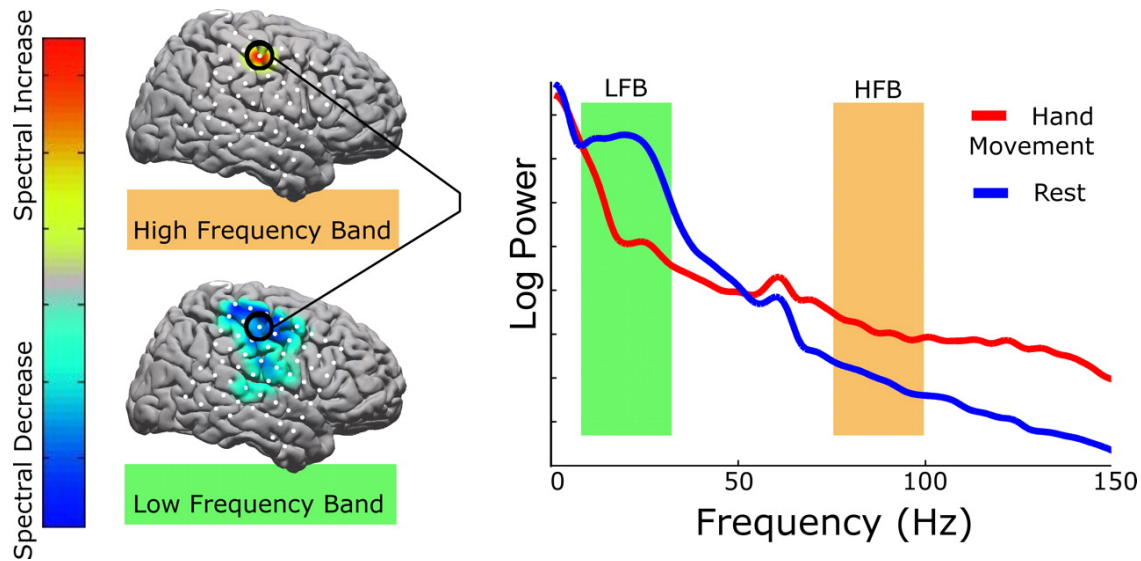


Figure 4: EEG power spectral bands for hand movement versus rest [63].

### 2.1.3 Other Implanted Electrodes

One of the earliest demonstrations of invasive BCI control in humans was using neurotrophic electrodes [45]. Neurotrophic electrodes consist of a 1-2 mm hollow glass cone attached to several gold conductive wires. The electrode is filled with trophic factors to encourage the growth of axons and dendrites into the cone [44]. Unique features of neurotrophic electrodes are their ability to isolate and record from single or small groups of neurons and their biocompatibility for long-term implantation [25]. However, compared to modern microelectrode arrays, neurotrophic electrodes have not been designed to conveniently sample larger numbers of neurons and have therefore not been widely adopted for BCI research.

More recently, an endovascular thin-film stent-electrode array was implanted in the superior sagittal sinus adjacent to the primary motor cortex of two participants with amyotrophic lateral sclerosis (ALS) [70]. This sensor array, known as a *stentrode*, consists of 17 circumferential sensors on a 8 mm  $\times$  40 mm monolithic, self-expanding nitinol scaffold designed for minimally invasive intracranial delivery using catheter venography. The array is connected to a 50 cm flexible transvascular lead and inserted into an inductively powered wireless

telemetry unit. For this feasibility study, the participants were able to successfully perform a typing task using attempted movements in combination with an eye-tracker for cursor navigation [70].

## 2.2 Noninvasive Recordings

The primary modality for noninvasive electrophysiological recordings of the brain is the scalp electroencephalogram (EEG). EEG is acquired via metallic electrodes placed directly on the scalp. EEG electrode diameters are generally on the order of centimeters and the number of electrodes used can be anywhere from 2, giving a single bipolar channel, to 256 - or even higher for detecting subcortical activity and source localization [80]. In order to provide conductivity through hair, the electrodes are either filled with electrolytic gel (i.e., wet electrodes) or have barbs designed to pass through hair (i.e., dry electrodes), as shown in Figure 2D.

Due to the signal attenuation caused by the skull and scalp layers, noninvasive recordings are lower in amplitude (10-100  $\mu\text{V}$ ) and are more prone to movement and muscle artifacts compared to invasive recordings. The use of active electrodes, which contain pre-amplifier circuitry embedded in the electrode housing, can effectively boost the signal and mitigate certain noise and artifacts in the recordings.

EEG signals for direct BCI control can broadly be categorized as *active* or *reactive* [102], depending on whether the brain activity is primarily modulated by endogenous or exogenous means, respectively.

### 2.2.1 Active Control Signals

The most commonly used active control signals for robotic control applications are event-related desynchronization/synchronization (ERD/ERS) [73] and sensorimotor rhythms (SMRs) [79]. These are more naturalistic control signals as they are generated from the motor cortex during actual and imagined movements.

SMRs are idling rhythms occurring in the alpha band of the motor cortex during rest, which can be observed in an estimated 80% of the population [79]. To distinguish from unrelated alpha band activity, these are often referred to as mu rhythms [3]. A defining characteristic of these rhythms is that the amplitude is attenuated over the corresponding area of the motor cortex during continued actual or imagined movements [72]. Related modulations can also be observed in the beta and gamma bands, although it is not clear whether these are contributed by distinct neural processes or are simply, in part, a byproduct of the unique temporal morphology of mu rhythms [58]. Users can learn to modulate SMR amplitudes continuously to achieve continuous, dimensional BCI control (e.g., imagine right hand movement to move a cursor to the right) [99]. The temporal, spatial, and spectral characteristics and how they can be mapped to dimensional BCI control are illustrated in Figure 5A.

ERD refers to the transient decrease in alpha-band power over the motor cortex associated with the onset of isolated movement or imagery, followed by the transient ERS increase as the motor activity returns to the resting state, as shown in Figure 5B. Thus, this transient activity can be used as a discrete switch, for instance to activate/deactivate a hand grasp orthotic [74].

Other active control signals exist, such as alpha-band modulation during cognitive processes such as mental math or object rotation [39, 91]. However, while these modulations can be reliably detected in the EEG, they require the user to perform a mental task that is not directly related to the primary robotic control task. This can be unnatural, unintuitive, and distracting, and is ultimately not an ideal control signal for a practical assistive device.

While ERD/ERS and SMR represent the most natural and intuitive scalp EEG activity for dimensional control of robotic or assistive devices, these signals tend to be non-stationary and significant task training may be required for users to reliably modulate these signals to achieve practical device control [57].

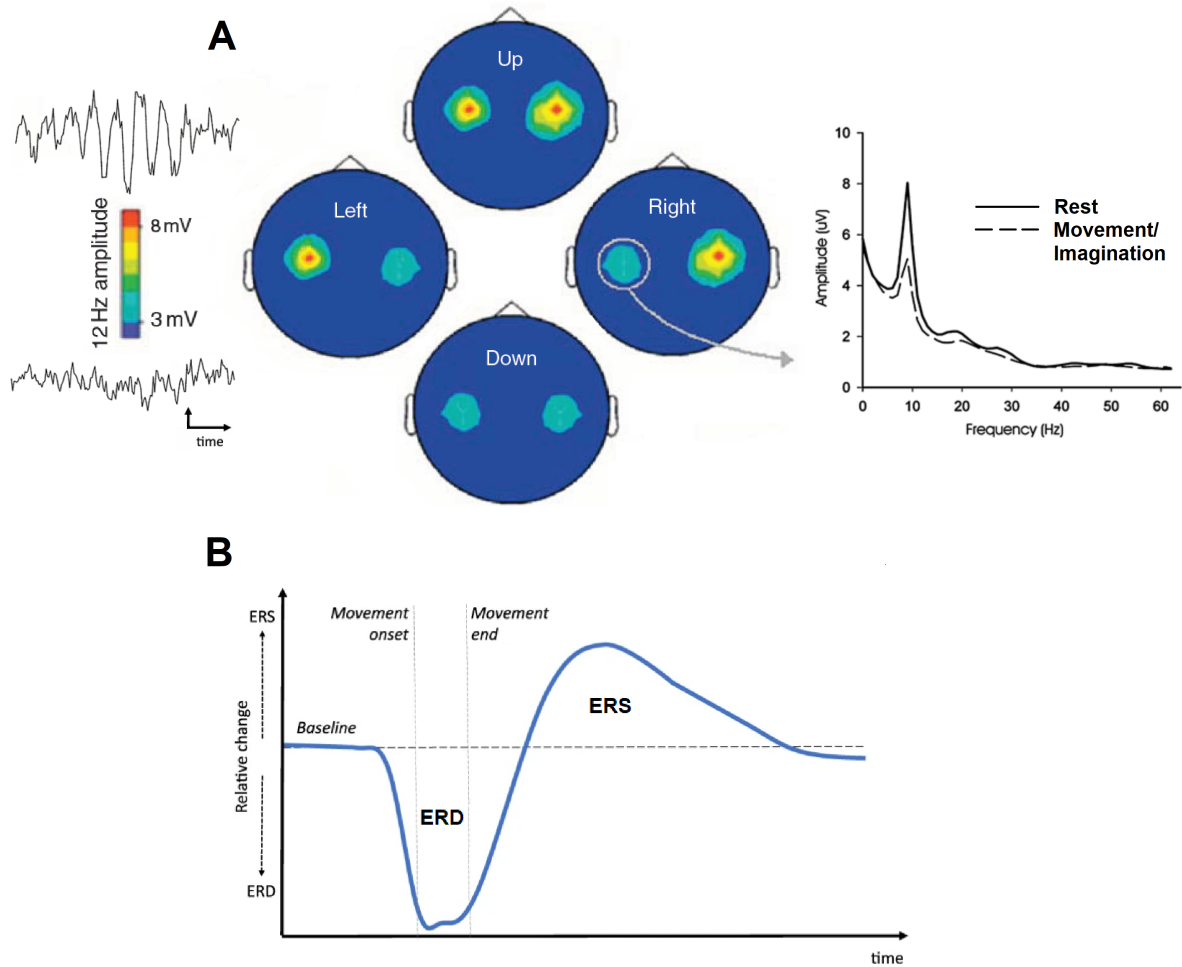


Figure 5: Active control signals. (A) Topographical and spectral representations of sensorimotor rhythms for dimensional control using left and right hand movement/imagery. (B) Event-related synchronization/desynchronization of the alpha band corresponding to an isolated movement/imagery.

### 2.2.2 Reactive Control Signals

Reactive control signals result from predictable changes in brain activity generated from the user's attention to specific sensory stimuli that are mapped to aspects of the control task [65]. These predictable changes in brain activity are known as stimulus-evoked potentials (SEPs). SEPs can either be transient, which are generally time-locked with the sensory stimulus and resolve on the order of a second, or steady-state, which continue as long as attention to the stimulus is maintained.

One of the earliest scalp EEG BCIs is the P300 Speller [22]. It operates based on the

brain's response to a rare or novel sensory stimulus. This brain response is known as an event-related potential (ERP), which is a specific type of SEP that includes a cognitive component (opposed to a purely sensory reflex). In this case, the cognitive component is the recognition that the stimulus is rare or novel.

In a simple P300 Speller paradigm, the user is presented with a matrix of flashing symbols on a computer monitor, for instance, similar to a visual keyboard. The user attends to the desired symbol as each symbol is flashed in a random sequence. The general concept is illustrated in Figure 6. Because the user does not know when the desired symbol will be flashed, an ERP is generated when the symbol is flashed while the user maintains fixed attention. Multiple ERPs must be accumulated over multiple stimulus sequences to reliably represent the characteristic brain response and determine the desired symbol. This process can be made more efficient via row/column flashing [22], or a variety of other enhancements to the original paradigm [42, 86]. While the original P300 Speller paradigm was based on visual attention, auditory [24] or tactile [7] attention can also be utilized with decreased performance compared to visual paradigms.

Effectively, such paradigms provide discrete command selection, equivalent to a computer keyboard - albeit at a much slower rate ( $\sim 4$ -5 symbols per minute) [86]. These commands can be mapped to achieve discrete dimensional [103] or goal-oriented [40] control of a robot, for example.

To achieve continuous dimensional control, steady-state sensory evoked potentials can be used, the most practical being the steady-state visual evoked potential (SSVEP) [60]. Unlike transient evoked potentials resulting from a single stimulus event, the steady-state evoked potentials result from a repeating stimulus pattern, such as a blinking light. As such, rather than generating a transient EEG response, predictable, continuous repeating EEG patterns over the occipital cortex are generated with attention to the repeating stimulus patterns. These EEG patterns manifest as distinct spectral peaks in the frequency domain that can be reliably identified and tracked, in contrast to the time-domain techniques used to identify

transient evoked potentials.

A typical SSVEP interface consists of a spatial array of individual lights or symbols on a screen, each concurrently repeating with a unique temporal flashing pattern and mapped to a control command, as shown in Figure 6. When the user focuses attention to a specific light/symbol, the brain activity unique to that symbol is detected and the associated command is executed. In contrast to transient evoked potentials, the command can be maintained with continued attention to the stimulus and can be readily changed by shifting attention to a different stimulus to execute the associated control command in a continuous fashion. This can enable joystick-like dimensional control of a robotic device with latency on the order of 0.5-1 seconds [93]. It is also possible to achieve high communication rates with discrete selection via keyboard-like interface using SSVEP and related variants [6, 15]. As with transient responses, BCIs have been developed that utilize steady-state auditory [32] and tactile (somatosensory) [1] potentials.

Control paradigms that rely on visual evoked potentials have several limitations. Foremost, performance can drastically decrease with inability to control eye movements [8, 87], which is the case for many locked-in patients. Also, these interfaces often create a visual cacophony, can be unnatural, fatiguing, and can be distracting from the primary control task [92], which can make them inconvenient and impractical for long-term use.

## **3 Applications to Assistive Robotics and Prosthetics**

### **3.1 Upper-limb Prosthetics**

Foundational work exploring the application of BCI for control of robotic arms was first performed in animal models. In 1999, Chapin et al. showed how rats could position a single degree of freedom (DoF) robotic arm in real time using a BCI driven by neuronal population activity in the primary motor cortex and ventrolateral thalamus [13]. Just a year later, Wessberg et al. demonstrated an open-loop BCI for real-time control of 3 DoF robotic arms,

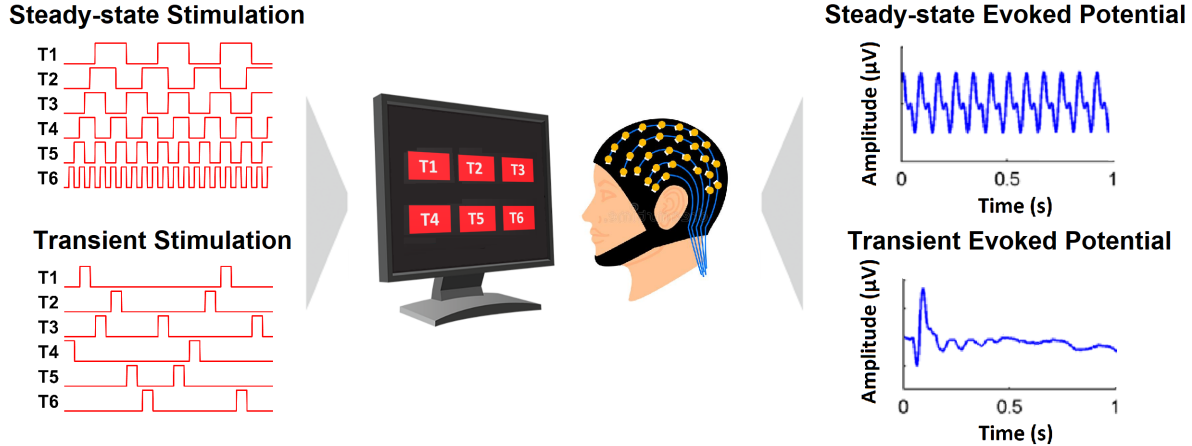


Figure 6: Reactive control signals for a visual paradigm. Six targets presented on a computer monitor flash independently according to (1) a steady-state pattern with a unique stimulus frequency for each target or (2) transient pulses with a unique stimulus onsets for each target. The user focuses visual attention on a single target and (1) the EEG over the occipital cortex oscillates at the target stimulus frequency (plus harmonics) for the steady-state stimulus scenario or (2) an EEG evoked potential can be detected over the visual cortex (and potentially other areas) with respect to the stimulus onset for the transient stimulus scenario.

which better represent the complex arm movements needed to accomplish a reach-and-grasp task [95]. In their approach, cortical neural ensemble activity, recorded from owl monkeys who received no feedback while completing reach-and-grasp tasks, was used to predict three-dimensional hand trajectories that controlled robotic movement. Further work succeeded in closing the loop for continuous neuronal control of robotic prostheses by non-human primates by introducing visual feedback, which resulted in stabilization of performance and more effective learning of neuromodulation [12, 52].

Velliste et al. demonstrated embodied control, involving real-time interaction with the physical environment, of a 4 DoF prosthetic arm using cortical signals in a closed loop system [88]. Modulation of cortical signals represented not only the velocity of the end effector in Cartesian space, but also the aperture velocity of the gripper’s fingers. This BCI enabled monkeys to continuously control the prosthetic device to reach to a food target, grasp the food, and then feed themselves. Physical interaction with the environment enabled displays of embodiment via behaviors inessential to task completion. For example, the monkey treated

the prosthetic arm as if it was its own by moving the gripper to its mouth in order to lick it instead of reaching to grasp the food target.

Initial results for BCI control of prosthetic devices by humans was demonstrated by Hochberg et al. in their report describing the first participant in a trial for BrainGate, a neuromotor prosthetic system consisting of a single cortically implanted, 96-channel sensor and external signal processors [33]. In this work, a patient with tetraplegia was enabled to grasp and move objects using a robotic arm controlled via neuronal ensemble spiking activity.

A follow up clinical trial of the BrainGate system, dubbed BrainGate2, showed how participants from the original BrainGate trial were able to use continuous neuronal ensemble control to operate a robotic arm for three-dimensional reach and grasp movements [34]. The BCI system enabled one participant with tetraplegia to, completely independently, manipulate and drink from a bottle for the first time in 14 years, as shown in Figure 7(left). The results from this work are achieved in participants whose intracortical arrays were implanted more than 5 years prior, which is promising evidence that the development of neural interfaces using chronically implanted intracortical sensors may be feasible.

Independent of the BrainGate trials, Collinger et al. demonstrated how a human with tetraplegia could control a 7 DoF prosthetic arm using an intracortical activity recorded from two, 96-channel arrays implanted in the motor cortex [17]. Continuous control was achieved by relating neural firing rates and movement velocity in each control dimension (3D translation, 3D orientation, 1D grasp) using a linear model, as previously demonstrated in non-human primate studies [88]. The participant was able to achieve both clinically significant improvement of function and complex, coordinated movements, on-par with that of able-bodied people, sustained over several weeks of testing. Figure 7B shows the participant feeding herself using the robotic arm.

In follow up work with the same patient, Wodlinger et al. expanded the 1D grasp, which simply allowed binary open/close, to now include four dimensions to control hand

shape, which introduced a new emphasis on object-interaction behavior [97]. The study demonstrated that object interaction during calibration of neural activity to intended control behaviors was important to achieve 10 dimensional operation of a prosthetic arm using the previously demonstrated linear model for neural decoding [17].

More recent work has considered the role of bidirectional BCI, which integrate both sensory and motor modalities for robust restoration of function [36], for the control of robotic arms [23, 76, 94]. Flesher et al. builds on previous demonstrations of high-dimensional continuous control of robotic arms using cortical activity and visual feedback alone [17, 97] by introducing tactile feedback [23]. Tactile percepts were evoked by intracortical microstimulation of the somatosensory cortex based on contact and grasp forces measured via sensors in the robotic arm, resulting in perceived tactile sensations at the palm and fingers. A participant with tetraplegia achieved higher performance when performing grasp-and-reach tasks, namely through reduction of grasp attempt time, with tactile sensation relative to that using BCI systems with only visual feedback.



Figure 7: Real-time BMI prosthetic arm control using microelectrode arrays implanted in the motor cortex. (Left) BrainGate [34]. (Right) University of Pittsburgh [17].

### 3.2 Orthotics and Exoskeletons

The application of BCI for the control of orthotics and exoskeletons has also been explored, often in the context of rehabilitation [54]. We restrict the scope of this chapter to focus only

on the control of orthotics or exoskeletons using BCI, not on the use and assessment of these systems for neurological rehabilitation.

One of the earliest demonstrations of BCI control of orthoses was by Pfurtscheller et al. [71]. Using a EEG based BCI, a tetraplegic patient was able to operate a hand orthosis. The participant was trained to modulate mu oscillations via a motor imagery approach, allowing the user to close or open the orthosis by imagining movement of their feet or hands, respectively. More recently, P300 based BCI systems for hand-orthosis control have also been demonstrated [82, 83]. Delijorge et al. [18] introduced a P300-based BCI to allow patients with amyotrophic lateral sclerosis (ALS) to control a robotic hand orthosis. Compared to previous work that only allows binary opening/closing of the hand [71, 82], this system enabled patients to control the movement of individual fingers.

EEG-based BCIs have also been demonstrated to control lower-limb exoskeletons. Kwak et al. [49, 50] presented an asynchronous SSVEP-based BCI system that controlled a leg exoskeleton to provide healthy participants with support while walking forward, turning, sitting, and standing. The oscillatory nature of SSVEPs make them a reasonable candidate to decode user intention for exoskeleton control despite the poor signal-to-noise ratio in the EEG signal caused by the introduction of additional artifacts while walking or broadband distortion by the exoskeleton. SSVEP based control of lower limb prostheses has been replicated by Wang et al. [90]. In the same study, motor imagery based control was also demonstrated and high accuracy performance was achieved by both approaches. In an approach that can be directly applied to knee orthoses, Murphy et al. presented ERD-based control to lock and unlock a prosthetic knee for the swing phase of gait or for sitting [67].

In an initial clinical proof-of-concept, Benabid et al. [5] showed how an individual with tetraplegia could control a four-limb, 14 DoF exoskeleton using an ECoG-based BCI. This exoskeleton is depicted in Figure 8. ECoG signals were recorded from the upper limb sensorimotor areas of the brain using two, epidural recorders implanted bilaterally. The number of degrees of freedom the patient was able to control increased gradually with training over a

period of 20 months, culminating in the ability to perform multi-limb action to complete 8D, bimanual tasks. Over the total 24 month length of the study, recalibration of the BCI was only required after considerably long intervals of time — more than 1.5 months. The results of this study suggest that ECoG may be a promising modality to enable higher dimensional control of exoskeletons by individuals with tetraplegia.

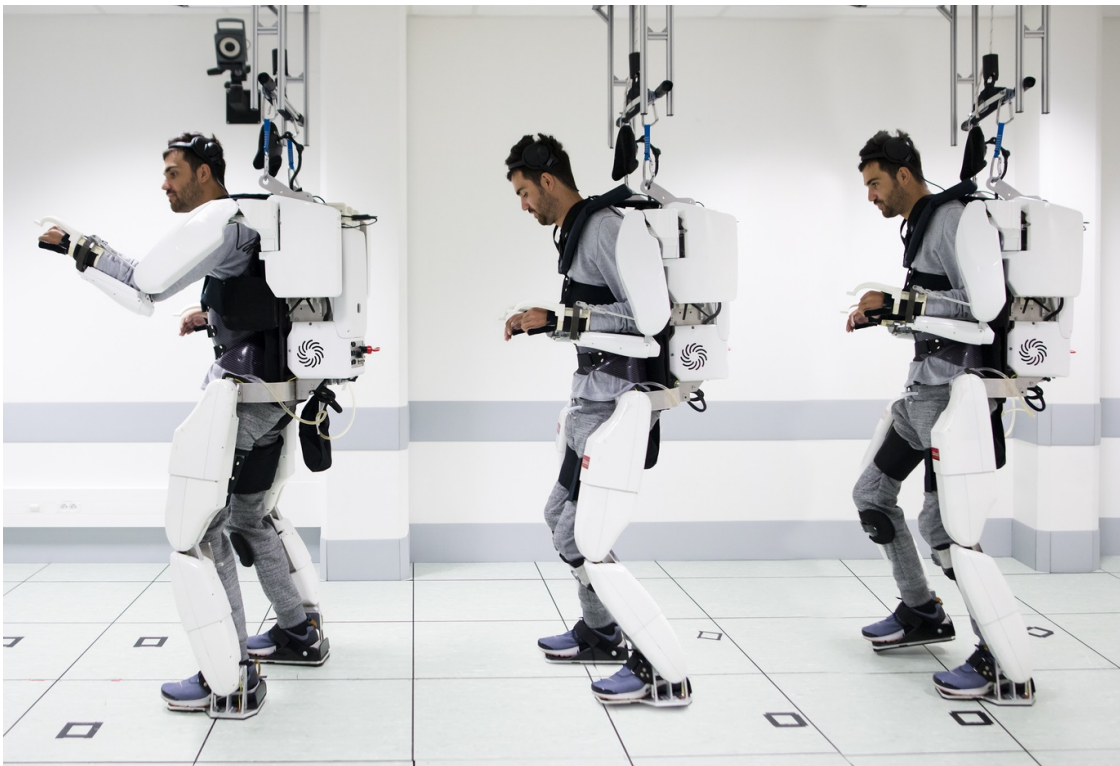


Figure 8: BCI-controlled exoskeleton. Quadriplegic individual moves with the assistance of robotic arms and legs controlled by decoding motor cortex activity in real-time. The brain signals are recorded with two 64-electrode ECoG implants [5].

### 3.3 Wheelchairs, Telepresence, and Assistive Robots

BCI controlled wheelchairs have the potential to improve the mobility of individuals with disabilities or movement disorders. Previously demonstrated BCI wheelchairs have largely been noninvasive, including P300 [37, 77], motor imagery [10, 84], or ERD/ERS [35] based paradigms. In the motor imagery approach developed by Carlson and Millan [10], the user was able to provide turning commands via the BCI system to a forward moving wheelchair

equipped with automatic obstacle avoidance.

Waytowich and Krusienski [93] introduced a SSVEP-based BCI, utilizing signals recorded from 5-channel dry-electrode EEG, for continuous control of a motorized wheelchair. Stimuli were superimposed over a live video feed of the environment, presented on an Android phone mounted in front of the user’s face, and were placed on the peripheral edges of the screen, as shown in Figure 9D. This approach allows the user to observe both the control stimuli and the environment in front of them with latencies on the order of 0.5-1 second.

While control of prosthetic or assistive robots generally focuses on allowing users to interact with their local environment, telepresence BCI systems can enable users to interact with their global environment through a remotely controlled robotic device. noninvasive telepresence BCI systems have been demonstrated to control a variety of devices including quadcopters [51], wheelchairs [93] (Figure 9C), robotic arms [95], humanoid robots [4], and mobile robots [11, 53, 61], among others. Millan et al. [61] showed how a mobile robot could be controlled using an asynchronous EEG-based BCI system to move between rooms of a simulated house. To achieve precise control despite the low bit rate of the EEG-based BCI, the user’s brain activity was associated with high level commands executed autonomously by the robot based on a behavior-based controller. BCI control of the mobile robot achieved similar task performance to manual control.

In this section, we distinguish BCI control of robotic arms as upper-arm prosthetics from their usage as assistive robots. As previously described, the former aims to achieve high-dimensional, continuous control that mimics natural function, typically using invasive BCI systems that decode cortical activity to control joint velocities. On the other hand, the latter consists of noninvasive BCI systems for goal oriented or partially automated control [28, 40, 56]. For example, Johnson et al. achieved high level control of a 6 DoF robotic arm using an adapted P300 Speller interface [40], as shown in Figure 9A. This goal-oriented approach leverages the discrete selection capabilities of P300 Spellers, allowing users to select a target for the robot’s end effector to move to its workspace, represented as a 4x4

grid. Similar to Waytowich et al. [93], an SSVEP approach was applied for continuous control of a robotic arm for a real-time writing application [28] (Figure 9B).

Some research has considered how near-continuous high-dimensional control of robotic arms can be achieved using noninvasive BCI systems. Meng et al. demonstrated a non-invasive ERD/ERS-based approach to control a robotic arm to complete three-dimensional reach and grasp tasks [59]. High accuracy continuous control of a device in 3D space requires the user to have three independent pairs of motor strategies, which has not been robustly demonstrated using noninvasive EEG-based BCI alone, although some previous work used 3D gaze tracking in combination with SMR-based BCI to achieve such control [69]. This study achieved the same outcomes of fluid 3D control through the combination of two sequential low dimensional control commands. In this approach, the user first continuously controls the end effector within a 2D plane to hover above some target object. Then, the 2D end effector position is held constant by the system while the user controls the end effector in the third dimension to complete the grasp. This two-step approach, while more time consuming than 3D fluid control, is able to achieve 3D reach-and-grasps while reducing the number of DoF the noninvasive BCI needs to simultaneously interpret.

## 4 Artificial Intelligence and Shared Control

Artificial intelligence employs sensors and processing algorithms to make decisions in response to environmental variables, often being implemented to adapt and learn new behaviors. Due to a variety of factors, such as limitations of brain activity sensing technologies, the current state of BCI control generally does not allow for perfectly precise and reliable execution of device commands. In particular, as the primary input for direct device control, current scalp-based EEG BCIs are generally slower and less reliable than using any residual volitional muscle movement as a simple binary control switch, for instance, especially for safety-critical applications. Thus, scalp-based BCIs are generally only practical for individ-

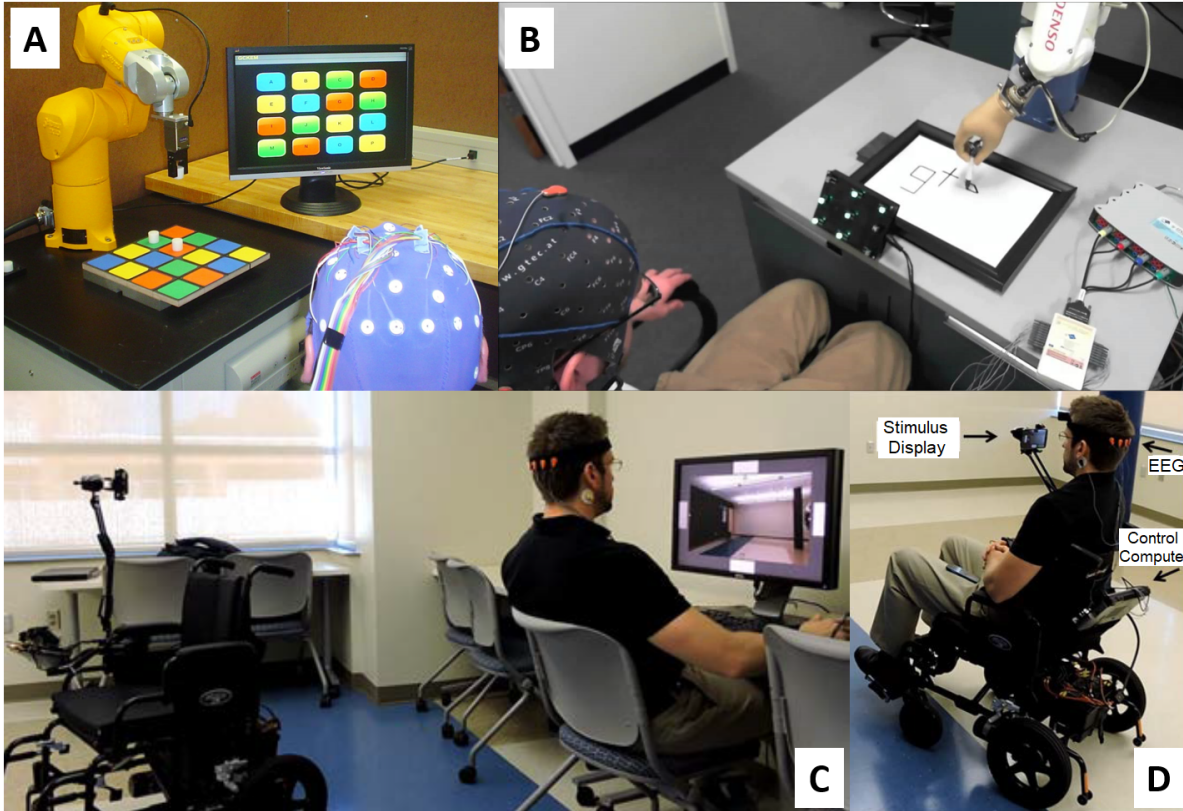


Figure 9: EEG-based robotics control. (A) Goal-oriented control of a pick-and-place robotic arm via a P300 paradigm [40]. (B) Continuous, real-time control of a robotic arm for writing via an SSVEP paradigm [28]. (C) Continuous, real-time control of a telepresence robot (remotely operated wheelchair with streaming camera view) via a remote SSVEP paradigm [93]. (D) Continuous, real-time control of a motorized wheelchair via an SSVEP paradigm displayed on a handheld device including pass-through camera view [93].

uals that are in or nearing a locked-in state without volitional muscle control, such as those suffering from late-stage ALS or brain-stem stroke [98]. Furthermore, for individuals in this state, the practical applications of robotic control become significantly more limited and specialized in terms of meeting their immediate basic needs.

To help mitigate the limitations of BCI as the primary controller, artificial intelligence can be employed to achieve shared control where some aspects of the robotic control are learned and automated by the machine, such as obstacle avoidance, trajectory planning, object interactions, balancing, etc., while other aspects such as navigation or goal-oriented commands, for instance, remain under the user’s direct control. This can provide interac-

tions that are more functional, natural, convenient, and/or less demanding for the user. In this context, the degree of shared control can range from full user (BCI) control to full autonomous (AI) control, with the relative proportion of user control depending on the nature and constraints of the application. Additionally, it is possible to dynamically vary the degree of user control depending on task demands and user workload, for example.

Depending on the application, artificial intelligence implementations can use a variety of sensing modalities mounted on or in proximity to the robot to acquire data for building a model of the environment. Such sensors may include cameras, optical sensors, accelerometers, ultrasonic sensors, and pressure sensors, for example.

Artificial intelligence is generally achieved via machine learning algorithms that implement supervised, unsupervised, or reinforcement learning strategies [47]. Supervised learning is when the system is trained using labeled data that corresponds to predefined states, actions, goals, etc. Unsupervised learning is when the data is not labeled, either because labels are not available or do not exist. Thus, unsupervised learning must find consistent patterns in the data to create or infer labels. Reinforcement learning can be applied when there are multiple approaches for achieving the same end goal. Here, specific actions are associated with a reward or penalty and, based on accumulated experience, the system learns appropriate sequences of actions to achieve the desired outcome by maximizing rewards and/or minimizing penalties.

Intelligent shared control has been implemented using a variety of strategies. For example, error-related potentials (ErrPs), ERPs that occur in response to observed errors [48], have been introduced as a feedback signal to train intelligent controllers to achieve optimal behaviors for a given task. Interactive reinforcement learning using ErrPs as implicit feedback has been shown for human-robot interaction (HRI) [46], including for co-adaptation in HRI [21]. ErrPs have also been used to teach neuroprostheses optimal control policies for goal-directed movement, allowing users to give high-level commands that the trained policy develops low-level plans to execute [38].

Computer vision based strategies for shared control have also been demonstrated [85, 101]. Muelling et al. [66], introduced a shared control framework that combines computer vision, intent prediction, and human-robot control arbitration to reduce perceived difficulty when using BCI to control a 7 DoF robotic arm. Vision based target-pose estimation can enable the robot to autonomously grasp targets once a person has moved its end effector close to the target via BCI control [101]. Applying target prediction in tandem with target-pose estimation allowed a shared controller to infer user intent and dynamically optimize user control commands to provide corrections while reaching or to autonomously grasp or place an object [9].

In the context of wheelchair control and mobile manipulators, shared controllers are often used to autonomously move to a user defined location in space [37], to assist with obstacle avoidance during user control [10], or some combination of these two approaches [19, 20, 30]. More recent approaches have considered how to dynamically modify when or to what extent wheelchair behavior is commanded by the human user or by a robot controller. Deng et al. showed how a Bayesian shared BCI system for wheelchair control can intelligently arbitrate human and robot control commands generated via kinematic modeling and vision-based path planning [19]. Building off of this work, Deng et al. [20] propose a self-adaptive self control system that evaluates subject’s control ability from single trial SSVEP to modify the level of assistance provided by the robot for wheelchair control.

## 5 Current Challenges and Future Prospects

With the aim of restoring natural function via a neuroprosthetic device (i.e., high DoF, continuous control), which will generally require invasive recordings from a large number of individual neurons, the existing challenges are distinctly different compared to that of a low DoF assistive device that can be achieved via noninvasive means. For the former, population coding has proven to very reliably decode movement trajectories for motor prosthetics.

However, there are still open questions regarding the practicality and long-term viability of current approaches [75], particularly with respect to the surgical risks. Furthermore, to move toward a fully-transparent motor prosthetic, information from an increasing number of neurons must be incorporated. Significant efforts are going into the development of high-density recording devices [41, 68], including practical implantation and long-term stability considerations. Access to larger numbers of neurons requires new and improved large-scale decoding algorithms which will, in turn, require additional behavioral data for training. Furthermore, to better model natural neuroplasticity in the brain, such models would likely need to be capable of adaptation, requiring data from appropriately designed closed-loop experiments. Because the user must also adapt to the model feedback, a precarious co-adaptation scenario is created for which closed-loop experiments would need to carefully examine the nature, timing, dynamics, and accuracy of the feedback [16].

Another critical consideration for developing fully-natural motor prosthetics is the integration of sensory feedback, including tactile, visual, proprioceptive, etc [23]. This requires a bi-directional BCI capable of providing coordinated and localized brain stimulation, which further complicates the aforementioned issues of electrode densities, locations, adaptive model development, and closed-loop experiments.

For lower-DoF assistive noninvasive devices, as mentioned in Section 4, the primary limitation lies with the practicality and fidelity of noninvasive recordings - particularly if the user has any residual volitional muscle control. Thus, such BCIs are generally only practical for locked-in users and the development of improved goal-oriented and shared-control methods holds the most promise until significant advances are made in noninvasive recording technologies. However, it must also be recognized that, as the BCI moves further toward goal-oriented or shared control, the user may lose a sense of agency relative to when they have truly continuous control. Otherwise, noninvasive BCIs do hold promise for motor rehabilitation [54], as well as potential integration of passive cognitive-state estimates such as cognitive workload, attention, affect, etc. into the BCI feedback control loop [2].

Overall, the BCI field is rapidly advancing and is beginning to receive serious commercial and investor interest, which is further accelerating the advances. With the recent developments in large-scale neural recording modalities and machine learning methods to handle the resulting ‘big data’, practical BCI-controlled motor prosthetics, exoskeletons, and assistive robotics for disabled end-users will become an eventual reality.

## References

- [1] S. K. Ahn, K. Kim, and S. C. Jun. Steady-state somatosensory evoked potential for brain-computer interface present and future. *Frontiers in Human Neuroscience*, 9, 2016.
- [2] M. Alimardani and K. Hiraki. Passive brain-computer interfaces for enhanced human-robot interaction. *Frontiers in Robotics and AI*, 7, 2020.
- [3] S. Arroyo, R. Lesser, B. Gordon, S. Uematsu, D. Jackson, and R. Webber. Functional significance of the mu rhythm of human cortex: an electrophysiologic study with subdural electrodes. *Electroencephalography and clinical neurophysiology*, 87 3:76–87, 1993.
- [4] C. J. Bell, P. Shenoy, R. Chalodhorn, and R. P. N. Rao. Control of a humanoid robot by a noninvasive brain-computer interface in humans. *Journal of neural engineering*, 5 2:214–20, 2008.
- [5] A. Benabid, T. Costecalde, A. Eliseyev, G. Charvet, A. Verney, S. Karakas, M. Foerster, A. Lambert, B. Moriniere, N. Abroug, M. Schaeffer, A. Moly, F. Sauter-Starace, D. Ratel, C. Moro, N. Torres-Martinez, L. Langar, M. Oddoux, M. Polosan, S. Pezzani, V. Auboiron, T. Aksenova, C. Mestais, and S. Chabardès. An exoskeleton controlled by an epidural wireless brain-machine interface in a tetraplegic patient: a proof-of-concept demonstration. *The Lancet Neurology*, 18:1112–1122, 2019.
- [6] G. Bin, X. Gao, Y. Wang, B. Hong, and S. Gao. VEP-based brain-computer interfaces: time, frequency, and code modulations. *IEEE Computational Intelligence Magazine*, 4, 2009.
- [7] A. Brouwer and J. B. F. Erp. A tactile P300 brain-computer interface. *Frontiers in Neuroscience*, 4, 2010.
- [8] P. Brunner, S. Joshi, S. Briskin, J. Wolpaw, H. Bischof, and G. Schalk. Does the ‘P300’ speller depend on eye gaze? *Journal of neural engineering*, 7 5:056013, 2010.
- [9] L. Cao, G. Li, Y. Xu, H. Zhang, X. Shu, and D. Zhang. A brain-actuated robotic arm system using non-invasive hybrid brain-computer interface and shared control strategy. *Journal of Neural Engineering*, 18, 2021.

- [10] T. Carlson and J. R. Millán. Brain-controlled wheelchairs: A robotic architecture. *IEEE Robotics & Automation Magazine*, 20:65–73, 2013.
- [11] T. Carlson, L. Tonin, S. Perdakis, R. Leeb, and J. R. Millán. A hybrid BCI for enhanced control of a telepresence robot. *2013 35th Annual International Conference of the IEEE Engineering in Medicine and Biology Society (EMBC)*, pages 3097–3100, 2013.
- [12] J. Carmena, M. Lebedev, R. Crist, J. O’Doherty, D. Santucci, D. Dimitrov, P. Patil, C. Henriquez, and M. Nicolelis. Learning to control a brain–machine interface for reaching and grasping by primates. *PLOS Biology*, 1, 2003.
- [13] J. K. Chapin, K. A. Moxon, R. S. Markowitz, and M. A. L. Nicolelis. Real-time control of a robot arm using simultaneously recorded neurons in the motor cortex. *Nature Neuroscience*, 2:664–670, 1999.
- [14] R. Chen, A. Canales, and P. Anikeeva. Neural recording and modulation technologies. *Nature reviews. Materials*, 2 2, 2017.
- [15] X. Chen, Y. Wang, M. Nakanishi, X. Gao, T. Jung, and S. Gao. High-speed spelling with a noninvasive brain–computer interface. *Proceedings of the National Academy of Sciences*, 112:E6058 – E6067, 2015.
- [16] G. Cheng, S. K. Ehrlich, M. Lebedev, and M. A. L. Nicolelis. Neuroengineering challenges of fusing robotics and neuroscience. *Science Robotics*, 5, 2020.
- [17] J. Collinger, B. Wodlinger, J. Downey, W. Wang, E. Tyler-Kabara, D. Weber, Angus JC McMorland, M. Velliste, M. Boninger, and A. Schwartz. High-performance neuroprosthetic control by an individual with tetraplegia. *The Lancet*, 381:557–564, 2013.
- [18] J. Delijorge, O. Mendoza-Montoya, J. L. Gordillo, R. Caraza, H. R. Martinez, and J. Antelis. Evaluation of a P300-based brain-machine interface for a robotic hand-orthosis control. *Frontiers in Neuroscience*, 14, 2020.
- [19] X. Deng, Z. L. Yu, C. Lin, Z. Gu, and Y. Li. A bayesian shared control approach for wheelchair robot with brain machine interface. *IEEE Transactions on Neural Systems and Rehabilitation Engineering*, 28:328–338, 2020.
- [20] X. Deng, Z. L. Yu, C. Lin, Z. Gu, and Y. Li. Self-adaptive shared control with brain state evaluation network for human-wheelchair cooperation. *Journal of neural engineering*, 2020.
- [21] S. K. Ehrlich and G. Cheng. Human-agent co-adaptation using error-related potentials. *Journal of neural engineering*, 15 6:066014, 2018.
- [22] L. Farwell and E. Donchin. Talking off the top of your head: toward a mental prosthesis utilizing event-related brain potentials. *Electroencephalography and clinical neurophysiology*, 70 6:510–23, 1988.

- [23] S. N. Flesher, J. Downey, J. Weiss, C. L. Hughes, A. Herrera, E. Tyler-Kabara, M. Boninger, J. Collinger, and R. Gaunt. A brain-computer interface that evokes tactile sensations improves robotic arm control. *Science*, 372:831 – 836, 2021.
- [24] A. Furdea, S. Halder, D. J. Krusienski, D. Bross, F. Nijboer, N. Birbaumer, and A. Kübler. An auditory oddball (p300) spelling system for brain-computer interfaces. *Psychophysiology*, 46 3:617–25, 2009.
- [25] M. Gearing and P. R. Kennedy. Histological confirmation of myelinated neural filaments within the tip of the neurotrophic electrode after a decade of neural recordings. *Frontiers in Human Neuroscience*, 14, 2020.
- [26] A. P. Georgopoulos, A. Schwartz, and R. Kettner. Neuronal population coding of movement direction. *Science*, 233 4771:1416–9, 1986.
- [27] V. Gilja, C. Pandarinath, C. H. Blabe, P. Nuyujukian, J. Simeral, A. Sarma, B. L. Sorice, J. Perge, B. Jarosiewicz, L. Hochberg, K. Shenoy, and J. Henderson. Clinical translation of a high-performance neural prosthesis. *Nature Medicine*, 21:1142–1145, 2015.
- [28] gtec medical engineering. <https://www.youtube.com/watch?v=8eOSlzDdOpg>. *YouTube*, Jul 2011.
- [29] M. A. Gull, S. Bai, and T. Bak. A review on design of upper limb exoskeletons. *Robotics*, 9:16, 2020.
- [30] X. Han, K. Lin, S. Gao, and X. Gao. A novel system of SSVEP-based human-robot coordination. *Journal of neural engineering*, 16 1:016006, 2019.
- [31] C. Herff, D. Krusienski, and P. Kubben. The potential of stereotactic-EEG for brain-computer interfaces: Current progress and future directions. *Frontiers in Neuroscience*, 14, 2020.
- [32] H. Higashi, T. M. Rutkowski, Y. Washizawa, A. Cichocki, and T. Tanaka. EEG auditory steady state responses classification for the novel BCI. *2011 Annual International Conference of the IEEE Engineering in Medicine and Biology Society*, pages 4576–4579, 2011.
- [33] L. Hochberg, M. Serruya, G. Friehs, J. A. Mukand, M. Saleh, A. Caplan, A. Branner, D. Chen, R. Penn, and J. Donoghue. Neuronal ensemble control of prosthetic devices by a human with tetraplegia. *Nature*, 442:164–171, 2006.
- [34] L. R. Hochberg, D. Bacher, B. Jarosiewicz, N. Y. Masse, J. D. Simeral, J. Vogel, S. Haddadin, J. Liu, S. S. Cash, P. Smagt, and J. P. Donoghue. Reach and grasp by people with tetraplegia using a neurally controlled robotic arm. *Nature*, 485:372 – 375, 2012.

- [35] D. Huang, K. Qian, D. Y. Fei, W. Jia, X. Chen, and O. Bai. Electroencephalography (EEG)-based brain-computer interface (BCI): A 2-d virtual wheelchair control based on event-related desynchronization/synchronization and state control. *IEEE Transactions on Neural Systems and Rehabilitation Engineering*, 20:379–388, 2012.
- [36] C. L. Hughes, A. J. Herrera, R. A. Gaunt, and J. L. Collinger. Bidirectional brain-computer interfaces. *Handbook of clinical neurology*, 168:163–181, 2020.
- [37] I. Iturrate, J. M. Antelis, A. Kübler, and J. Minguez. A noninvasive brain-actuated wheelchair based on a P300 neurophysiological protocol and automated navigation. *IEEE Transactions on Robotics*, 25:614–627, 2009.
- [38] I. Iturrate, R. Chavarriaga, L. Montesano, J. Minguez, and J. R. Millán. Teaching brain-machine interfaces as an alternative paradigm to neuroprosthetics control. *Scientific Reports*, 5, 2015.
- [39] C. Jeunet, B. N’Kaoua, S. Subramanian, M. Hachet, and F. Lotte. Predicting mental imagery-based BCI performance from personality, cognitive profile and neurophysiological patterns. *PLoS ONE*, 10, 2015.
- [40] G. D. Johnson, N. R. Waytowich, D. Cox, and D. J. Krusienski. Extending the discrete selection capabilities of the P300 speller to goal-oriented robotic arm control. *2010 3rd IEEE RAS & EMBS International Conference on Biomedical Robotics and Biomechatronics*, pages 572–575, 2010.
- [41] J. Jun, N. A. Steinmetz, J. H. Siegle, D. J. Denman, M. Bauza, B. Barbarits, A. K. Lee, C. A. Anastassiou, A. Andrei, Ç. Aydın, M. Barbic, T. J. Blanche, V. Bonin, J. Couto, B. Dutta, S. L. Gratiy, D. A. Gutnisky, M. Häusser, B. Karsh, P. Ledochowitsch, C. M. Lopez, C. Mitelut, S. Musa, M. Okun, M. Pachitariu, J. Putzeys, P. D. Rich, C. Rossant, W. Sun, K. Svoboda, M. Carandini, K. D. Harris, C. Koch, J. O’Keefe, and T. D. Harris. Fully integrated silicon probes for high-density recording of neural activity. *Nature*, 551:232–236, 2017.
- [42] T. Kaufmann, S. Schulz, C. Grünzinger, and A. Kübler. Flashing characters with famous faces improves ERP-based brain-computer interface performance. *Journal of neural engineering*, 8 5:056016, 2011.
- [43] S. S. Kellis, P. House, K. Thomson, R. Brown, and B. Greger. Human neocortical electrical activity recorded on nonpenetrating microwire arrays: applicability for neuroprostheses. *Neurosurgical focus*, 27 1:E9, 2009.
- [44] P. Kennedy. The cone electrode: a long-term electrode that records from neurites grown onto its recording surface. *Journal of Neuroscience Methods*, 29:181–193, 1989.
- [45] P. Kennedy, R. Bakay, M. Moore, K. Adams, and J. Goldwaithe. Direct control of a computer from the human central nervous system. *IEEE transactions on rehabilitation engineering : a publication of the IEEE Engineering in Medicine and Biology Society*, 8 2:198–202, 2000.

- [46] S. K. Kim, E. A. Kirchner, A. Stefes, and F. Kirchner. Intrinsic interactive reinforcement learning – using error-related potentials for real world human-robot interaction. *Scientific Reports*, 7, 2017.
- [47] O. Kroemer, S. Niekum, and G. D. Konidaris. A review of robot learning for manipulation: Challenges, representations, and algorithms. *J. Mach. Learn. Res.*, 22:30:1–30:82, 2021.
- [48] Akshay Kumar, Lin Gao, Elena Pirogova, and Qiang Fang. A review of error-related potential-based brain–computer interfaces for motor impaired people. *IEEE Access*, 7:142451–142466, 2019.
- [49] N. S. Kwak, K. R. Müller, and S. W. Lee. A lower limb exoskeleton control system based on steady state visual evoked potentials. *Journal of neural engineering*, 12 5:056009, 2015.
- [50] N. S. Kwak, K.-R. Muller, and Seong-Whan Lee. Toward exoskeleton control based on steady state visual evoked potentials. *2014 International Winter Workshop on Brain-Computer Interface (BCI)*, pages 1–2, 2014.
- [51] K. Lafleur, K. Cassady, A. Doud, K. Shades, E. Rogin, and B. He. Quadcopter control in three-dimensional space using a noninvasive motor imagery-based brain-computer interface. *Journal of neural engineering*, 10 4:046003, 2013.
- [52] M. Lebedev, J. Carmena, J. O’Doherty, M. Zacksenhouse, C. Henriquez, J. Principe, and M. Nicolelis. Cortical ensemble adaptation to represent velocity of an artificial actuator controlled by a brain-machine interface. *Journal of Neuroscience*, 25, 2005.
- [53] R. Leeb, L. Tonin, M. Rohm, L. Ferro Desideri, T. Carlson, and J. R. Millán. Towards independence: A BCI telepresence robot for people with severe motor disabilities. *Proceedings of the IEEE*, 103:969–982, 2015.
- [54] R. Mane, T. Chouhan, and C. Guan. BCI for stroke rehabilitation : motor and beyond. *Journal of neural engineering*, 2020.
- [55] E. M. Maynard, C. T. Nordhausen, and R. A. Normann. The utah intracortical electrode array: a recording structure for potential brain-computer interfaces. *Electroencephalography and clinical neurophysiology*, 102 3:228–39, 1997.
- [56] D. McFarland and J. Wolpaw. Brain-computer interface operation of robotic and prosthetic devices. *Computer*, 41, 2008.
- [57] D. McFarland and J. Wolpaw. Brain–computer interface use is a skill that user and system acquire together. *PLoS Biology*, 16, 2018.
- [58] D. J. McFarland, L. A. Miner, T. M. Vaughan, and J. R. Wolpaw. Mu and beta rhythm topographies during motor imagery and actual movements. *Brain Topography*, 12:177–186, 2004.

- [59] J. Meng, S. Zhang, A. Bekyo, J. Olsoe, B. Baxter, and B. He. Noninvasive electroencephalogram based control of a robotic arm for reach and grasp tasks. *Scientific Reports*, 6, 2016.
- [60] M. Middendorf, G. McMillan, G. Calhoun, and K. S. Jones. Brain-computer interfaces based on the steady-state visual-evoked response. *IEEE transactions on rehabilitation engineering : a publication of the IEEE Engineering in Medicine and Biology Society*, 8 2:211–4, 2000.
- [61] J.I R. Millán, F. Renkens, J. Mouriño, and W. Gerstner. Noninvasive brain-actuated control of a mobile robot by human EEG. *IEEE Transactions on Biomedical Engineering*, 51:1026–1033, 2004.
- [62] K. Miller, C. Honey, D. Hermes, Rajesh P. N. Rao, M. Nijs, and J. Ojemann. Broad-band changes in the cortical surface potential track activation of functionally diverse neuronal populations. *NeuroImage*, 85:711–720, 2014.
- [63] K. Miller, E. Leuthardt, G. Schalk, R. P. N. Rao, N. Anderson, D. Moran, J. W. Miller, and J. Ojemann. Spectral changes in cortical surface potentials during motor movement. *The Journal of Neuroscience*, 27:2424 – 2432, 2007.
- [64] K. J. Miller, L. B. Sorensen, J. G. Ojemann, and M. Nijs. Power-law scaling in the brain surface electric potential. *PLoS Computational Biology*, 5, 2009.
- [65] K. Misulis and T. Fakhoury. Spehlmann’s evoked potential primer. 2001.
- [66] K. Muelling, A. Venkatraman, J. S. Valois, J. E. Downey, J. M. Weiss, S. Javdani, M. Hebert, A. B. Schwartz, J. L. Collinger, and J. A. Bagnell. Autonomy infused teleoperation with application to brain computer interface controlled manipulation. *Autonomous Robots*, 41:1401–1422, 2017.
- [67] D. Murphy, O. Bai, A. S. Gorgey, J. Fox, W. Lovegreen, B. Burkhardt, R. Atri, J. S. Marquez, Q. Li, and D. Y. Fei. Electroencephalogram-based brain–computer interface and lower-limb prosthesis control: A case study. *Frontiers in Neurology*, 8, 2017.
- [68] E. Musk. An integrated brain-machine interface platform with thousands of channels. *Journal of Medical Internet Research*, 21, 2019.
- [69] G. Onose, C. Grozea, A. Anghelescu, C. Daia, C. J. Sinescu, A. V. Ciurea, T. Spiricu, A. Mirea, I. Andone, A. Spanu, C. Popescu, A. S. Mihăescu, S. Fazli, M. Danóczy, and F. Popescu. On the feasibility of using motor imagery EEG-based brain–computer interface in chronic tetraplegics for assistive robotic arm control: a clinical test and long-term post-trial follow-up. *Spinal Cord*, 50:599–608, 2012.
- [70] T. Oxley, P. Yoo, G. Rind, S. M. Ronayne, C. M. S. Lee, C. Bird, V. Hampshire, R. Sharma, A. Morokoff, D. Williams, C. Macisaac, M. Howard, L. Irving, I. Vrljic, C. J. Williams, S. E. John, F. Weissenborn, M. Dazenko, A. Balabanski, D. A. Friedenberg, A. Burkitt, Y. Wong, K. Drummond, P. Desmond, D. Weber, T. Denison,

- L. Hochberg, S. Mathers, T. J. O'Brien, C. May, J. Mocco, D. Grayden, B. Campbell, P. Mitchell, and N. Opie. Motor neuroprosthesis implanted with neurointerventional surgery improves capacity for activities of daily living tasks in severe paralysis: first in-human experience. *Journal of Neurointerventional Surgery*, 13:102 – 108, 2020.
- [71] G. Pfurtscheller, C. Guger, G. R. Müller, G. Krausz, and C. Neuper. Brain oscillations control hand orthosis in a tetraplegic. *Neuroscience Letters*, 292:211–214, 2000.
- [72] G. Pfurtscheller, C. Neuper, D. Flotzinger, and M. Pregenzer. EEG-based discrimination between imagination of right and left hand movement. *Electroencephalography and clinical neurophysiology*, 103 6:642–51, 1997.
- [73] G. Pfurtscheller and F. L. D. Silva. Event-related EEG/MEG synchronization and desynchronization: basic principles. *Clinical Neurophysiology*, 110:1842–1857, 1999.
- [74] G. Pfurtscheller, T. Solis-Escalante, R. Ortner, P. Linortner, and G. Muller-Putz. Self-paced operation of an SSVEP-based orthosis with and without an imagery-based “brain switch:” a feasibility study towards a hybrid BCI. *IEEE Transactions on Neural Systems and Rehabilitation Engineering*, 18:409–414, 2010.
- [75] V. S. Polikov, P. A. Tresco, and W. M. Reichert. Response of brain tissue to chronically implanted neural electrodes. *Journal of Neuroscience Methods*, 148:1–18, 2005.
- [76] K. M. Quick, J. M. Weiss, F. Clemente, R. A. Gaunt, and J. L. Collinger. Intracortical microstimulation feedback improves grasp force accuracy in a human using a brain-computer interface\*. *2020 42nd Annual International Conference of the IEEE Engineering in Medicine & Biology Society (EMBC)*, pages 3355–3358, 2020.
- [77] B. Rebsamen, E. Burdet, C. Guan, H. Zhang, C. L. Teo, Q. Zeng, M. H. Ang, and C. Laugier. A brain-controlled wheelchair based on P300 and path guidance. *The First IEEE/RAS-EMBS International Conference on Biomedical Robotics and Biomechanics, 2006. BioRob 2006.*, pages 1101–1106, 2006.
- [78] G. Schalk and E. Leuthardt. Brain-computer interfaces using electrocorticographic signals. *IEEE Reviews in Biomedical Engineering*, 4:140–154, 2011.
- [79] D. Schomer and F. L. D. Silva. Niedermeyer’s electroencephalography: Basic principles, clinical applications, and related fields. 2010.
- [80] M. Seeber, L. Cantonas, M. Hoevens, T. Sesia, V. Visser-Vandewalle, and C. Michel. Subcortical electrophysiological activity is detectable with high-density EEG source imaging. *Nature Communications*, 10, 2019.
- [81] J. Shih, D. Krusienski, and J. Wolpaw. Brain-computer interfaces in medicine. *Mayo Clinic proceedings*, 87 3:268–79, 2012.
- [82] A. Stan, D. Irimia, N. Botezatu, and R. Lupu. Controlling a hand orthosis by means of P300-based brain computer interface. *2015 E-Health and Bioengineering Conference (EHB)*, pages 1–4, 2015.

- [83] N. Syrov, K. A. Novichikhina, D. A. Kir’yanov, S. Y. Gordleeva, and A. Y. Kaplan. The changes of corticospinal excitability during the control of artificial hand through the brain–computer interface based on the P300 component of visual evoked potential. *Human Physiology*, 45:152–157, 2019.
- [84] K. Tanaka, K. Matsunaga, and H. O. Wang. Electroencephalogram-based control of an electric wheelchair. *IEEE Transactions on Robotics*, 21:762–766, 2005.
- [85] J. Tang and Z. Zhou. A shared-control based BCI system: For a robotic arm control. *2017 First International Conference on Electronics Instrumentation & Information Systems (EIIS)*, pages 1–5, 2017.
- [86] G. Townsend, B. K. LaPallo, C. Boulay, D. Krusienski, G. E. Frye, C. K. Hauser, N. E. Schwartz, T. Vaughan, J. Wolpaw, and E. Sellers. A novel P300-based brain–computer interface stimulus presentation paradigm: Moving beyond rows and columns. *Clinical Neurophysiology*, 121:1109–1120, 2010.
- [87] M. Treder and B. Blankertz. Covert attention and visual speller design in an ERP-based brain-computer interface. *Behavioral and Brain Functions : BBF*, 6:28 – 28, 2010.
- [88] M. Velliste, S. Perel, M. Chance Spalding, A. S. Whitford, and A. B. Schwartz. Cortical control of a prosthetic arm for self-feeding. *Nature*, 453:1098–1101, 2008.
- [89] R. J. Vetter, J. C. Williams, J. F. Hetke, E. A. Nunamaker, and D. R. Kipke. Chronic neural recording using silicon-substrate microelectrode arrays implanted in cerebral cortex. *IEEE Transactions on Biomedical Engineering*, 51:896–904, 2004.
- [90] C. Wang, X. Wu, Z. Wang, and Y. Ma. Implementation of a brain-computer interface on a lower-limb exoskeleton. *IEEE Access*, 6:38524–38534, 2018.
- [91] Q. Wang and O. Sourina. Real-time mental arithmetic task recognition from EEG signals. *IEEE Transactions on Neural Systems and Rehabilitation Engineering*, 21:225–232, 2013.
- [92] N. R. Waytowich and D. Krusienski. Spatial decoupling of targets and flashing stimuli for visual brain-computer interfaces. *Journal of neural engineering*, 12 3:036006, 2015.
- [93] N. R. Waytowich and D. Krusienski. Development of an extensible SSVEP-BCI software platform and application to wheelchair control. *2017 8th International IEEE/EMBS Conference on Neural Engineering (NER)*, pages 259–532, 2017.
- [94] S. M. Wendelken, D. M. Page, T. S. Davis, H. A. C. Wark, D. T. Kluger, C. C. Duncan, D. J. Warren, D. T. Hutchinson, and G. A. Clark. Restoration of motor control and proprioceptive and cutaneous sensation in humans with prior upper-limb amputation via multiple Utah slanted electrode arrays (USEAs) implanted in residual peripheral arm nerves. *Journal of NeuroEngineering and Rehabilitation*, 14, 2017.

- [95] J. Wessberg, C. R. Stambaugh, J. D. Kralik, P. D. Beck, M. Laubach, J. K. Chapin, J. B. Kim, S. J. Biggs, M. A. Srinivasan, and M. A. L. Nicolelis. Real-time prediction of hand trajectory by ensembles of cortical neurons in primates. *Nature*, 408:361–365, 2000.
- [96] F. Willett, Donald T. Avansino, L. Hochberg, J. Henderson, and K. Shenoy. High-performance brain-to-text communication via handwriting. *Nature*, 593 7858:249–254, 2021.
- [97] B. Wodlinger, J. E. Downey, E. C. Tyler-Kabara, A. B. Schwartz, M. L. Boninger, and J. L. Collinger. Ten-dimensional anthropomorphic arm control in a human brain-machine interface: difficulties, solutions, and limitations. *Journal of neural engineering*, 12 1:016011, 2015.
- [98] J. Wolpaw, N. Birbaumer, D. McFarland, G. Pfurtscheller, and T. Vaughan. Brain-computer interfaces for communication and control. *Clinical Neurophysiology*, 113:767–791, 2002.
- [99] J. Wolpaw and D. McFarland. Control of a two-dimensional movement signal by a noninvasive brain-computer interface in humans. *Proceedings of the National Academy of Sciences of the United States of America*, 101 51:17849–54, 2004.
- [100] J. Wolpaw and E. Wolpaw. Brain-computer interfaces: Principles and practice. 2012.
- [101] Y. Xu, H. Zhang, L. Cao, X. Shu, and D. Zhang. A shared control strategy for reach and grasp of multiple objects using robot vision and noninvasive brain-computer interface. *IEEE Transactions on Automation Science and Engineering*, pages 1–13, 2020.
- [102] T. Zander and Christian Kothe. Towards passive brain-computer interfaces: applying brain-computer interface technology to human-machine systems in general. *Journal of neural engineering*, 8 2:025005, 2011.
- [103] Jing Zhao, Wei Li, and Mengfan Li. Comparative study of ssvep- and p300-based models for the telepresence control of humanoid robots. *PLoS ONE*, 10, 2015.